International Journal of Heat and Mass Transfer 53 (2010) 990–996

Contents lists available at ScienceDirect

International Journal of Heat and Mass Transfer

journal homepage: www.elsevier.com/locate/ijhmt

A critical evaluation of force term in lattice Boltzmann method, natural convection problem

A.A. Mohamad *, A. Kuzmin

Department of Mechanical and Manufacturing Engineering, Schulich School of Engineering, University of Calgary, 2500 University Drive NW, Calgary, Alta., Canada T2N 1N4

ARTICLE INFO

Article history:
Received 3 July 2009
Received in revised form 24 October 2009
Accepted 24 October 2009
Available online 1 December 2009

Keywords:
Lattice boltzmann method
Natural convection
Force term implementation

ABSTRACT

Few methods have been introduced and used in simulation fluid flows using lattice Boltzmann method (LBM) with external forces, such as buoyancy, surface tension, magnetic, etc. In some problems, the external force is constant, for instance gravitational force with constant density flows, while for other problems the force may vary spatially and/or temporally with non-zero gradients, such as gravitational force with variable density flows. For problems with the variable force term, adding force term to LBM may not be trivial. The paper evaluates mainly three different schemes of adding force term to LBM with BGK method. In this work, natural convection in a closed and an open ended cavities were used as a test platform. The results for the differentially heated cavity are introduced first. For the open cavity, the vertical left hand wall of the cavity is heated and opposing side is opened to the ambient, with other connecting boundaries are assumed to be adiabatic. Prior to the solution, the boundary conditions at the opening are unknown. The results of predictions using LBM are compared with results predicted by using finite volume method (FVM). The results are presented for $Ra = 10^6$ and for $Pr = 0.71$. It is found that most methods suggested in the literature produces similar results, despite that some authors claim that their scheme is more accurate than the other schemes.

1. Introduction

No need to say that lattice Boltzmann methods (LBM) is in high pace development and became a powerful method for simulation fluid flows and transport problems for single [1] and multi-phase flows [2]. However, there are many issues needed more investigations and critical evaluations. Also, the method is used by some authors with less attention to the limitations and constrains of the parameters in LBM. One of these issues is the proper treatment of the external forces, which is the topic of the present paper.

Luo [3] suggested that the force term can be introduced into the collision term as

$$F_i = -3\omega_i \rho \mathbf{c}_i.\mathbf{F}/c^2, \tag{1}$$

which is similar to that adopted for lattice gas model [4].

Shan and Chen [5] suggested to introduce the body force to the collision operator as

$$F_i = -3w_i\left(\frac{\mathbf{c}_i - \mathbf{u}}{c^2} + 3\frac{\mathbf{c}_i \cdot \mathbf{u}}{c^4}\mathbf{c}_i\right) \cdot \mathbf{F}. \tag{2}$$

Luo [6] showed that Eq. (1) is special case of Eq. (2). Buick and Greated [7] reviewed a few techniques for dealing with force (source) term for LBM. Also, they introduced a modified method. They concluded that the best results can be obtained by adding the force term to the collision process as

$$F_i = \frac{4}{c^2}\left(1 - \frac{1}{2\tau}\right)\mathbf{F} \cdot \mathbf{c}_i, \tag{3}$$

and the equilibrium velocity should be calculated as,

$$\mathbf{u}(\mathbf{x}, t) = \frac{1}{\rho}\sum_i \mathbf{c}_i f_i(\mathbf{x}, t) + \frac{\mathbf{F}\Delta t}{2\rho}. \tag{4}$$

The claim was based on testing few previously introduced methods by using Poiseuille flow as a benchmark, where the analytical result is easy to obtain.

Guo et al. [8] analyzes showed that by simple adding force term to the collision process and without shifting the velocity field neither in calculating of the equilibrium distribution function nor in calculating of the macroscopic velocity, here we called Scheme I, is not appropriate. Also, Guo et al. [8] argued that the methods introduced by Martys and Shan [9] and luo [6,10] are not appropriate for a non-constant body force problems. The method of Luo [6] and Martys and Shan [9] modified the collision process by adding force term as in Eq. (2) without shifting velocity field. Also, Guo et al. [8] mentioned that method introduced by Ladd and Verberg [11] should have better accuracy and generality compared with other examined methods. Furthermore, Guo et al. [8] stated that

* Corresponding author.
E-mail addresses: mohamad@ucalgary.ca (A.A. Mohamad), shurik.kuzmin@gmail.com (A. Kuzmin).

0017-9310/$ - see front matter © 2009 Elsevier Ltd. All rights reserved.
doi:10.1016/j.ijheatmasstransfer.2009.11.014

the method of Buick and Greated [7], which is mentioned before, does not correctly derive the momentum equation. Guo et al. [8] analyzes showed the method suggested by them is the best representative of continuity and momentum equations on the macroscopic scale, i.e., Navier–Stokes equation. [8] method, here called Scheme III, is to introduce the force population in the collision process as

$$F_i = w_i\left(1-\frac{1}{2\tau}\right)\left[\frac{\boldsymbol{c}_i-\boldsymbol{u}}{c_s^2}+\frac{\boldsymbol{c}_i(\boldsymbol{c}_i\cdot\boldsymbol{u})}{c_s^4}\right]\boldsymbol{F} \tag{5}$$

and to shift the equilibrium and macroscopic velocity fields as

$$\boldsymbol{u} = \frac{1}{\rho}\sum_i \boldsymbol{c}_i f_i + \frac{\boldsymbol{F}\Delta t}{2\rho}. \tag{6}$$

In the literature, the most popular methods are either adding extra force term to the collision term (Scheme I) or by modifying the velocity field with force term using Newton 2nd law (Scheme II). It should be mentioned that Buick and Greated [7] and Guo et al. [8] used the Poiseuille flow problem as a test platform. We think that natural convection problem is an ideal candidate for testing force term for two reasons. First, the body force is the function of temperature, and the temperature is variable throughout the domain. Second, there is a coupling between momentum equation and energy equation, hence the macroscopic velocity field is used in solving the energy equation. Therefore, inappropriate calculation of the macroscopic velocity field results in the incorrect temperature field. Natural convection in a differentially heated cavity is considered in this paper. The problem is used by CFD community in testing macroscopic solvers. Natural convection in a differentially heated cavity should show skew-symmetry in streamlines and isotherms plots for steady state solution, otherwise the solution is not fully converged. Also, the temperature at the centre of the cavity must be the average temperature of the heated and cold vertical boundaries, i.e., equal to 0.5 in non-dimensional scale; and the velocity at the centre must be zero. Furthermore, the rate of heat transfer in the differentially heated cavity is available in the open literature.

In the following sections, most popular methods of adding external force to LBM will be examined and discussed, namely three Schemes I, II and III. Furthermore, natural convection in an open ended cavity is also examined. The problem is very interesting, where the flow is driven by buoyancy force induced by the heated left hand wall, while the cavity is open to the ambient condition on the other end (right hand vertical wall). The other connecting boundaries are assumed to be adiabatic, Fig. 1. The boundary conditions (velocity components and temperature) at the open end are unknown prior to solution at the boundary. Mohamad et al. [12] solved this problem using LBM, and results were compared with finite volume method (FVM). The problem is interesting because the body force is non-uniform and asymmetric.

2. Governing equations

Standard D2Q9, LBM method is used in this work; hence only brief discussion will be given in the following paragraphs, for completeness. The BGK approximation lattice Boltzmann equation with external forces can be written as

$$f_i(\boldsymbol{x}+\boldsymbol{c}_i\Delta t, t+\Delta t) - f_i(\boldsymbol{x},t) = -\frac{f_i(\boldsymbol{x},t)-f_i^{eq}(\boldsymbol{x},t)}{\tau} + \Delta t F_i, \tag{7}$$

where f_i are the particle distributions defined for the finite set of the discrete particle velocity vectors $\boldsymbol{c}_i$, $\tau = \frac{1}{\omega_m}$ is the relaxation time, f_i^{eq} is the local equilibrium distribution function that has an appropriately prescribed functional dependence on the local hydrodynamic properties. In the above equation F_i is the force component in the ith direction. The equilibrium distribution can be formulated as

$$f_i^{eq} = w_i\rho\left[1+3\frac{\boldsymbol{c}_i\boldsymbol{u}^{eq}}{c^2}+\frac{9}{2}\frac{(\boldsymbol{c}_i\boldsymbol{u}^{eq})^2}{c^4}-\frac{3}{2}\frac{\boldsymbol{u}^{eq}\boldsymbol{u}^{eq}}{c^2}\right], \tag{8}$$

where $\boldsymbol{u}^{eq}$ and ρ are the velocity and the density used in the calculation of the equilibrium distribution function, respectively. We need to differentiate between two kinds of velocities, velocities used to calculate the equilibrium distribution function ($\boldsymbol{u}^{eq}$) and macroscopic velocity ($\boldsymbol{u}_m$). This is important because some authors define different values for each of the mentioned velocities. w_i are the weighting factors, for D2Q9 are given as

$$w_i = \begin{cases} 4/9 & i=0,\ \text{rest particle} \\ 1/9 & i=1,2,3,4 \\ 1/36 & i=5,6,7,8 \end{cases} \tag{9}$$

The discrete velocities, $\boldsymbol{c}_i$, for the D2Q9 (Fig. 2) are defined as follows:

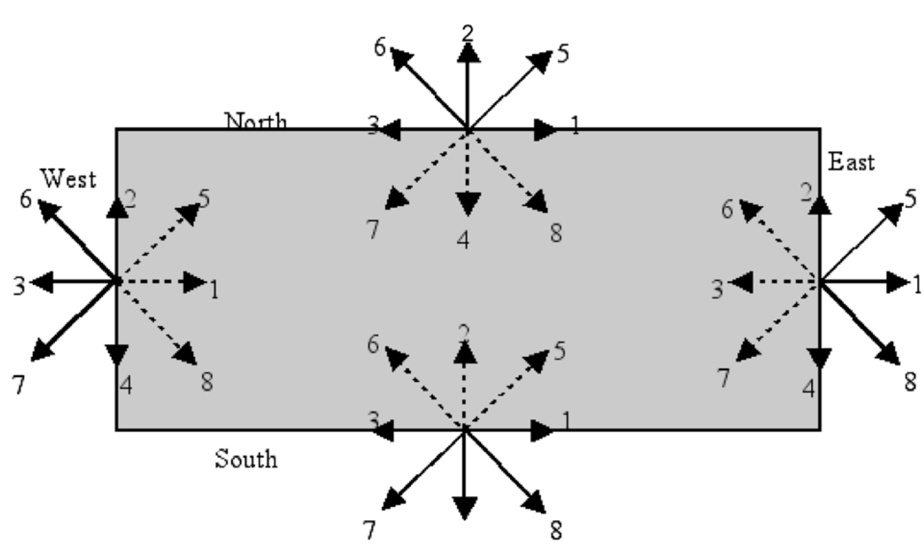

Fig. 1. Boundary conditions with unknown and known populations.

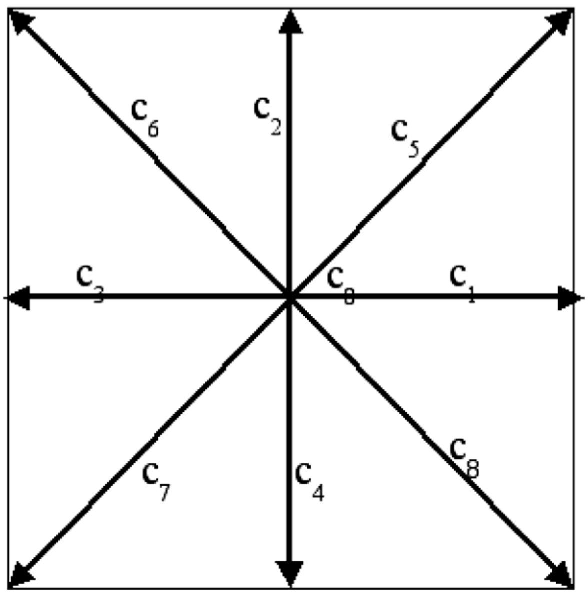

Fig. 2. D2Q9 velocities.

$$\boldsymbol{c}_i = \begin{cases} \boldsymbol{c}_0 = (0,0) & \\ \boldsymbol{c}_i = c(\cos\theta_i, \sin\theta_i) & \theta_i = (i-1)\pi/2 \\ & i = 1,2,3,4 \\ \boldsymbol{c}_i = c\sqrt{2}(\cos\theta_i, \sin\theta_i) & \theta_i = (i-5)\pi/2 + \pi/4 \\ & i = 5,6,7,8 \end{cases} \tag{10}$$

where $c = \Delta x/\Delta t$, Δx and Δt are the lattice space and the lattice time step size, respectively, which are set to unity. The basic hydrodynamic quantities, such as density ρ and velocity $\boldsymbol{u}$, are obtained through moment summations in the velocity space (without external force term):

$$\begin{aligned} \rho(\boldsymbol{x},t) &= \sum_i f_i(\boldsymbol{x},t) \\ \rho\boldsymbol{u}(\boldsymbol{x},t) &= \sum_i \boldsymbol{c}_i f_i(\boldsymbol{x},t) \end{aligned} \tag{11}$$

The macroscopic viscosity is determined by

$$\nu = \left(\tau - \frac{1}{2}\right)c_s^2\Delta t, \tag{12}$$

where c_s is the lattice speed of sound in media, and it equals to $c/\sqrt{3}$.

3. Force term

For natural convection driven flow, the force term is:

$$\boldsymbol{F} = \rho\boldsymbol{g}\beta\Delta T, \tag{13}$$

where $\boldsymbol{g}$ is the gravitational vector, ρ is the density, ΔT is the temperature difference between hot and cold boundaries and β is the thermal expansion coefficient.

There are a few methods suggested in the literature in adding source or force term to LBM. In this work we consider most commonly used Schemes (I and II) and compare them with the scheme suggested by Guo et al. [8] (III).

I – The force term added to the collision process as:

$$F_i = w_i\boldsymbol{F}.\boldsymbol{c}_i/c_s^2 \tag{14}$$

and the velocity field is not shifted, i.e., $\boldsymbol{u} = \boldsymbol{u}^{eq} = \boldsymbol{u}_{\boldsymbol{m}}$.

II – The velocity field is shifted as

$$\boldsymbol{u}(\boldsymbol{x},t) = \frac{1}{\rho}\sum_i \boldsymbol{c}_i f_i(\boldsymbol{x},t) + \frac{\boldsymbol{F}\tau}{\rho} \tag{15}$$

which is based on Newton's second law. For this scheme no force term is added to the collision process and $\boldsymbol{u} = \boldsymbol{u}^{eq} = \boldsymbol{u}_m$.

III – Guo scheme:

$$F_i = w_i\left(1 - \frac{1}{2\tau}\right)\left[\frac{\boldsymbol{c}_i - \boldsymbol{u}}{c_s^2} + \frac{\boldsymbol{c}_i(\boldsymbol{c}_i \cdot \boldsymbol{u})}{c_s^4}\right] \cdot \boldsymbol{F} \tag{16}$$

The above term needs to be added into the collision process also the velocity need to be shifted as

$$\boldsymbol{u}^{eq} = \frac{1}{\rho}\sum_i \boldsymbol{c}_i f_i + \frac{\boldsymbol{F}\Delta t}{2\rho} \tag{17}$$

and

$$\boldsymbol{u}_m = \frac{1}{\rho}\sum_i \boldsymbol{c}_i f_i + \frac{\boldsymbol{F}\Delta t}{2\rho}, \tag{18}$$

where $\boldsymbol{u}^{eq} = \boldsymbol{u}_m$.

4. Method of solution

For natural convection problem we have two sets of distribution functions – one for density and velocity, defined above, and another is needed for the temperature field [1,13–15]. Since, viscous heating effects and compression work are negligible, both of the distribution functions are coupled through the following force term:

$$\boldsymbol{F} = \rho\boldsymbol{g}\beta(T - T_{ref}), \tag{19}$$

where ρ is the local density, β is the thermal expansion coefficient, T is the local temperature, and T_{ref} is the reference temperature, cold wall or ambient temperature, usually set to 0 in the non-dimensional scale. The buoyancy force couples the Navier–Stokes equation with energy equation. For Navier–Stokes equation D2Q9 model is used, while for temperature distribution D2Q4 model is used. For D2Q4 the LBE can be written as

$$g_i(\boldsymbol{x} + \boldsymbol{c}_i, t + \Delta t) = g_i(\boldsymbol{x},t)[1 - \omega_s] + \omega_s g_i^{eq}(\boldsymbol{x},t) \tag{20}$$

The equilibrium distribution functions for temperature is as follows

$$g_i^{eq} = w_i T(x,t)\left[1 + \frac{\boldsymbol{c}_i.\boldsymbol{u}}{c_s^2}\right] \tag{21}$$

For details we refer to [1]. It should mention that, D2Q4 simulates advection diffusion equation (energy equation) accurately. Also, the heat fluxes predicted by D2Q4 were well compared with prediction of Navier Stokes solver (finite volume method). Notice that ω is different for the momentum and the temperature equations. For momentum ω_m is prescribed through kinematic viscosity as

$$\omega_m = \frac{1}{3\nu + 0.5} \tag{22}$$

For the temperature or energy equation, the ω_s is related to diffusion coefficient as

$$\omega_s = \frac{1}{2\alpha + 0.5}, \tag{23}$$

where α is the thermal diffusion coefficient. Local Nusselt number is calculated as

$$Nu = \frac{\partial\theta}{\partial X} \tag{24}$$

Nusselt number is based on H, which is the cavity height. In the above equation θ stands for non-dimensional temperature,

$\theta = (T - T_{ref})/\Delta T$, where $\Delta T = (T_{hot} - T_{ref})$. Average Nusselt number is calculated as

$$Nu_{av} = \frac{1}{M} \sum_{k=1}^{k=M} \frac{\partial \theta}{\partial x} \tag{25}$$

where M is total number of lattices in y-direction. For instance, the average Nusselt number at the hot wall is

$$Nu_{av} = \frac{1}{M} \sum_{k=1}^{k=M} \frac{\theta_w - \theta_{w+1}}{\Delta x} N \tag{26}$$

where N is the number of lattices in x-direction, θ_w and θ_{w+1} are wall temperature and temperature at the lattice adjacent to the wall, respectively.

5. Boundary conditions

In LBM distribution functions out of the domain are known from the streaming process. The unknown distribution functions are those towards the domain. Fig. 1 shows the unknown distribution functions, which are needed to be determined, as dotted lines. Fig. 3 shows the schematics of the problem with coordinate system and boundary conditions.

5.1. Density distribution function

For the density distribution functions, bounce-back boundary conditions were applied on all solid boundaries, which means that incoming boundary populations equal to out-going populations after the collision. For instance for west boundary, the following conditions are imposed:

$$\begin{aligned} f_1(x,y) &= \tilde{f}_3(x,y) \\ f_5(x,y) &= \tilde{f}_7(x,y) \\ f_8(x,y) &= \tilde{f}_6(x,y) \end{aligned} \tag{27}$$

where $\tilde{f}_i$ represents the distribution function after collision and streaming, similarly for other boundaries. For open boundary, east boundary, first order interpolation is used, i.e.

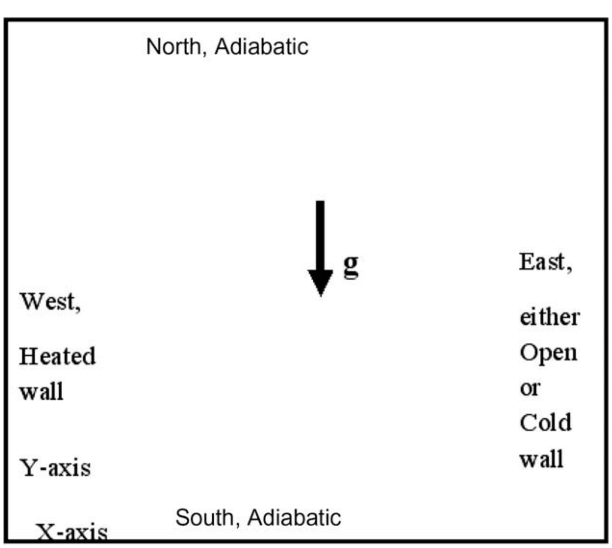

Fig. 3. Boundary conditions and domain presentation.

$$\begin{aligned} f_3(n,y) &= \tilde{f}_3(n-1,y) \\ f_6(n,y) &= \tilde{f}_6(n-1,y) \\ f_7(n,y) &= \tilde{f}_7(n-1,y) \end{aligned} \tag{28}$$

where n is the lattice at the boundary and $n-1$ is the lattice in the domain neighbor to the boundary lattice.

5.2. Temperature distribution function

For the temperature distribution function, bounce back is used for adiabatic boundaries (north and south boundaries). For the heated wall, west boundary, flux conservation equation is applied [16], i.e.

$$g_1(0,y) - g_1^{eq}(0,y) + g_3(0,y) - g_3^{eq}(0,y) = 0 \tag{29}$$

Since g^{eq} at the wall is equal to $w_i\theta_w$, then $g^{eq} = 0.25\theta_w$. The above equation can be formulated as

$$g_1(0,y) = 0.5 - g_3(0,y) \tag{30}$$

For east cold wall $\theta = 0$, then $g_3(n,y) = -g_1(n,y)$.

For the open boundary, east boundary, the boundary condition depends on the x-direction velocity. If the flow is entering the domain from the ambient then the dimensionless temperature, θ, should be zero. If the flow is leaving the domain, then the temperature is extrapolated, i.e.

$$g_3(n,y) = g_3(n-1,y) \tag{31}$$

6. Method of solution

The standard LBM consists of two steps, collision and streaming. D2Q9 is used to solve for the velocity field, and D2Q4 is used to solve for the temperature field. Lattices (100×100 and 150×150) are used in x- and y-direction. By fixing Rayleigh number and Prandtl number, the viscosity and thermal diffusivity are calculated from definition of Reynolds and Prandtl numbers. Eqs. (22) and (23) are used to calculate the relaxation times for density and temperature distribution functions. Viscosity is selected to insure that Mach number is within the limit of incompressible flow. For the buoyant flow, the magnitude velocity is order of

$$u = \sqrt{g\beta \triangle TM} \tag{32}$$

where M is number of lattices in y-direction (parallel to gravitational acceleration). Rayleigh and Prandtl numbers are defined as $Ra = \frac{g\beta\Delta TM^3}{\alpha\upsilon}$, and $Pr = \upsilon/\alpha$, respectively . Hence, Eq. (24) can be reformulated as

$$u = \sqrt{\frac{Ra\upsilon^2}{M^2 Pr}} \tag{33}$$

The Mach number, $Ma = u/c = \sqrt{\frac{Ra\upsilon^2}{M^2 Prc^2}}$. For instance, for $Ra = 10^6$, $Pr = 0.71$, $\upsilon = 0.01$, $c = 1/\sqrt{3}$ and for number of lattices in y-direction, M = 100, the Ma will be about 0.042, which is much less than 0.3 (incompressibility limit). The thermal diffusion coefficient, α, is calculated from definition of Pr, i.e., $\alpha = \upsilon/Pr$.

For all the examined schemes the following algorithm is used:

1. Calculate the equilibrium density distribution function.
2. Calculate the force population (if needed).
3. Perform the collision procedure with force term. The collision procedure perform for all lattices including lattice sites at the boundaries.
4. Stream the density distribution populations.
5. Apply boundary conditions for density distribution function.
6. Calculate macroscopic velocity field, shift velocity (if needed).

7. Calculate equilibrium velocity.
8. Calculate the equilibrium distribution function for the temperature.
9. Perform collision for the temperature distribution function.
10. Stream the temperature distribution populations.
11. Apply boundary conditions for the temperature.

Notice that the velocities that are used for calculation the equilibrium distribution function for the density and the temperature may be different. However, for the schemes mentioned in this work, both velocities are the same. However, the macroscopic velocity should be always utilized for calculating the temperature equilibrium distribution functions.

In the present work three different force implementations schemes are examined for natural convection problems. The schemes are:

1. Adding force term as a source (Scheme I).
2. Velocity shift (Scheme II).
3. Guo et al. [8] method of the implementation of the force term (Scheme III).

7. Results

The mentioned three schemes of implementing force term in LBM results were discussing in the following paragraphs. Rayleigh number is fixed to $Ra = 10^6$ and Pr is set to 0.71 (air).

Table 1 summarizes the average Nusselt number predicted by different schemes and for different value of ν and for lattice numbers of 100×100 and 150×150. All results are presented for the same number of iterations (time), 25,00,00. The average Nusselt number predicted by finite volume method (FVM) is about 8.825 [17], and temperature at the centre of the cavity should be 0.5. Comparing the results summarized in the table for the different schemes, it is clear that Scheme I does better job than the other two Schemes II and III in the sense that the center temperature is about 0.5. However, the average Nusselt numbers predicted by all tested schemes are comparable to the FVM prediction. Furthermore, Table 2 compared the results predicted by Scheme I with benchmark results published by , for U_{max}, V_{max} and their locations in vertical and horizontal mid planes (i.e., $X = 0.5$ and $Y = 0.5$, respectively). Fig. 4 shows time series for temperature at the centre of the cavity for 100×100 lattice and for two different ν values predicted by mentioned schemes. For $\nu = 0.01$, the difference between the predictions of the three schemes is not that significant. However, Scheme I prediction is more accurate compared with other two scheme. As the viscosity increased to 0.05, the errors

Table 1
Summary of average Nusselt number and dimensionless temperature at the centre of the cavity predicted by different schemes.

ν	Lattice	Nu_{aver}	Temperature
Scheme I:			
0.01	150×150	8.816–8.9075	0.498301
	100×100	8.652–8.9502	0.499896
0.05	150×150	8.259–8.8549	0.494866
	100×100	7.424–9.0134	0.483198
0.005	150×150	9.317–8.4542	0.468182
	100×100	8.750–8.8791	0.495397
Scheme II:			
0.01	150×150	8.8818–8.8308	0.493129
	100×100	8.8013–8.7763	0.488148
0.05	150×150	8.6754–8.4896	0.462672
	100×100	8.4705–7.9923	0.411520
0.005	150×150	9.3449–8.4207	0.465994
	100×100	8.8223–8.7922	0.489727
Scheme III:			
0.01	150×150	8.8781–8.8351	0.493412
	100×100	9.0866–8.7862	0.488028
0.05	150×150	8.5816–8.5775	0.469756
	100×100	8.2438–8.2260	0.426516
0.005	150×150	9.3440–8.4217	0.466043
	100×100	8.8203–8.7946	0.489887

Table 2
Comparison of LBM predictions (Scheme I) with Benchmark solution of [17] (number in the brackets).

Ra	U_{max}	Y_{max}	V_{max}	X_{max}	Nu_{av}
10^5	34.6755 (34.7399)	0.8516 (0.8553)	68.0494 (68.6396)	0.06968 (0.06602)	4.5707 (4.5264)
10^6	64.7348 (64.8367)	0.85517 (0.85036)	218.993 (220.461)	0.03996 (0.03887)	8.8765 (8.8251)

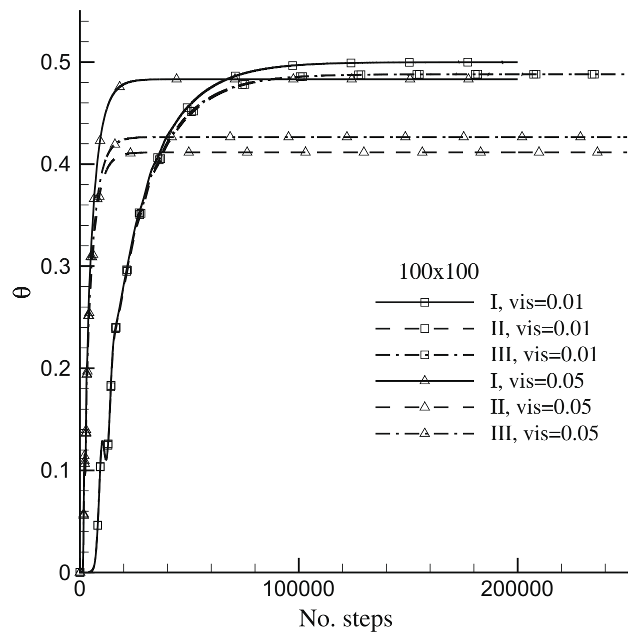

Fig. 4. Time series for temperature at the centre of the cavity for 100×100 lattice.

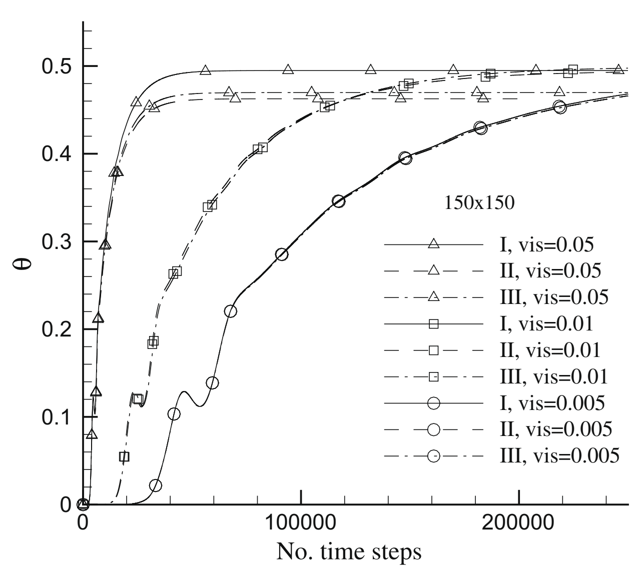

Fig. 5. Time series for temperature at the centre of the cavity for 150×150 lattice.

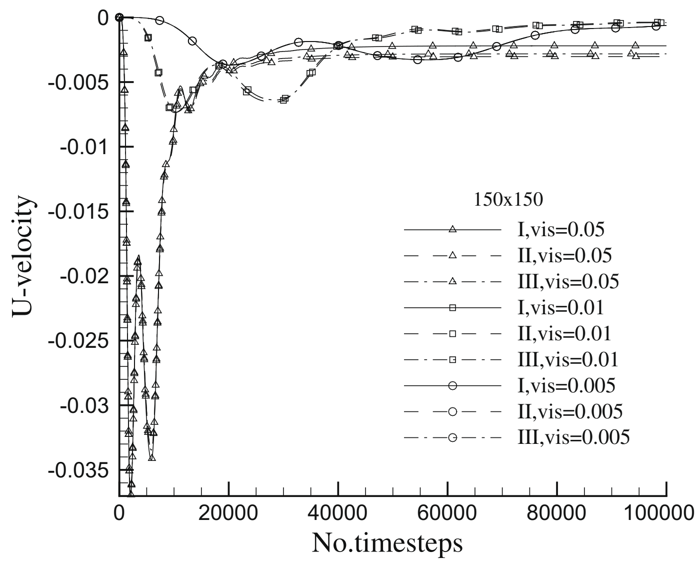

Fig. 6. Time series for velocity at the centre of the cavity for 150 × 150 lattice.

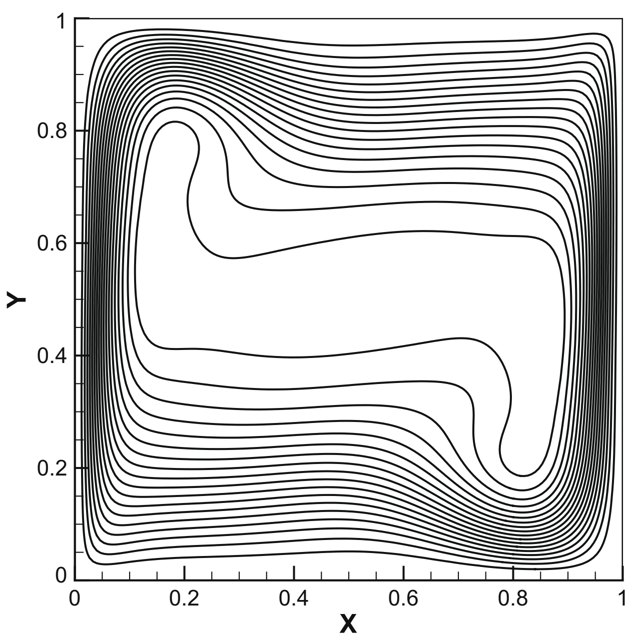

Fig. 7. Streamlines of the Scheme I.

in predictions of Schemes II and III are significantly increased. While, Scheme I does a better job. For instance, the errors in predictions of Schemes I, II and III are about 3.4%, 17.7% and 14.7 %, respectively, for $\nu = 0.05$. Increasing number of lattices to 150×150 shows that the difference between predictions of all schemes diminishes for ν less than 0.01, Fig. 5. For, $\nu = 0.05$, Scheme I again shows better predictions compared with other schemes predictions. The figure shows that as the ν decreases the number of time step needed to reach convergent solution (steady state solution) increases. This is expected because time scale is function of ν (relaxation time). Similar conclusions can be said about velocity component at the center of the cavity, Fig. 6. The velocity at the center of the cavity should be zero. The prediction of all schemes are consistent for $\nu \leqslant 0.01$. For $\nu = 0.05$, the error in predictions of Scheme I is relatively less than the predictions of the other schemes. Streamlines predicted by the Scheme I shows almost perfect skew symmetry, Fig. 7, which is consistent with benchmark solution. Other schemes showed similar results.

The results for open cavity also revealed that the predictions of Schemes II and III are almost the same. However, the predictions of Scheme I is slightly different. Fig. 8 shows the time series for the temperature at the centre of the cavity. Interested readers on results of open cavity, Ref. [12] may be consulted.

8. Conclusion

Three most commonly used schemes for implementing the source (force) term into LBM are tested and compared by using natural convection problem as a test platform. The results showed that adding force term to the collision process gives more accurate results. However, for small value of viscosity or high value of ω, all the tested schemes predicted the same results. We think that the

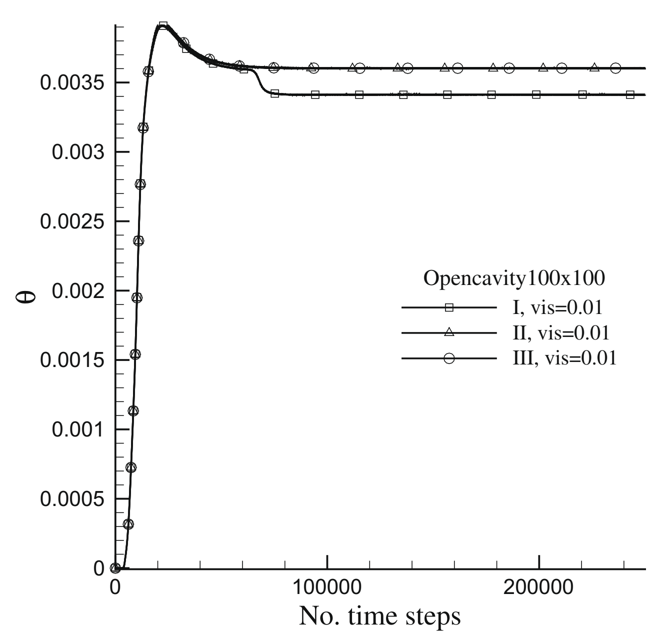

Fig. 8. Time series for temperature at the centre of the open cavity.

test platform used in this work is reliable candidate and results revealed that by adding the force term into the collision process is simple and hence is recommended.

References

[1] A.A. Mohamad, Applied Lattice Boltzmann Method for Transport Phenomena, Momentum, Heat and Mass Transfer, Sure Print, Calgary, 2007.
[2] S. Succi, The Lattice Boltzmann Equation for Fluid Dynamics and Beyond, Oxford University Press, Oxford, 2001.
[3] L.-S. Luo, Lattice-Gas Automata and Lattice Boltzmann Equations for Two-Dimensional Hydrodynamics, Ph.D. thesis, Georgia Institute of Technology, 1993.
[4] U. Frisch, D. d'Humieres, B. Hasslacher, P. Lallemand, Y. Pomeau, J.P. Rivet, Lattice gas hydrodynamics in two and three dimensions, Compl. Syst. 1 (4) (1987) 633–647.
[5] X. Shan, H. Chen, Simulation of nonideal gases and gas–liquid phase transitions by the lattice Boltzmann equation, Phys. Rev. E 49 (4) (1994) 2941–2948.
[6] L.-S. Luo, Unified theory of lattice Boltzmann models for non-ideal gases, Phys. Rev. Lett. 81 (8) (1998) 1618–1621.
[7] J.M. Buick, C.A. Greated, Gravity in a lattice Boltzmann model, Phys. Rev. E 61 (5) (2000) 5307–5320.
[8] Z. Guo, C. Zheng, B. Shi, Discrete lattice effects on the forcing term in the lattice Boltzmann method, Phys. Rev. E 65 (046308) (2002) 1–6.
[9] N.S. Martys, X. Shan, H. Chen, Evaluation of the external force term in the discrete Boltzmann equation, Phys. Rev. E 58 (5) (1998) 6855–6857.
[10] L.-S. Luo, Theory of the lattice Boltzmann method: lattice Boltzmann models for nonideal gases, Phys. Rev. E 62 (4) (2000) 4982–4996.
[11] A.J.C. Ladd, R. Verberg, Lattice-Boltzmann simulations of particle–fluid suspensions, J. Stat. Phys. 104 (5/6) (2001) 1191–1251.
[12] A.A. Mohamad, M. El-Ganaoui, R. Bennacer, Lattice Boltzmann simulation of natural convection in an open ended cavity, Int. J. Therm. Sci. 48 (10) (2009) 1870–1875.
[13] X. He, S. Chen, G. Doolen, A novel thermal model for the lattice Boltzmann method in incompressible limit, J. Comput. Phys. 146 (1998) 282–300.
[14] A. D'Orazio, M. Corcione, G.P. Celata, Application to natural convection enclosed flows of a lattice Boltzmann BGK model coupled with a general purpose thermal boundary condition, Int. J. Therm. Sci. 43 (6) (2004) 531–630.
[15] H.N. Dixit, V. Babu, Simulation of high Rayleigh natural convection in a square cavity using the lattice Boltzmann method, Int. J. Heat Mass Transfer 49 (2006) 727–739.
[16] Q. Zou, X. He, On pressure and velocity boundary conditions for the lattice Botlzmann BGK model, Phys. Fluids 9 (6) (1997) 1591–1598.
[17] M. Hortmann, M. Peric, G. Scheuerer, Finite volume multigrid prediction of laminar natural convection: bench-mark solutions, Int. J. Numer. Meth. Fluids 11 (1990) 189–207.